Electron-plasmon interactions in resonant molecular tunnel junctions

L. Adamska,[1] M. A. Kozhushner,[2] and I. I. Oleynik[1]
[1]*Department of Physics, University of South Florida, Tampa, Florida 33620, USA*
[2]*Institute of Chemical Physics, Russian Academy of Sciences, Kosygin St., 4, Moscow 119991, Russia*
(Received 7 October 2009; published 6 January 2010)

In this paper, we show that electron-plasmon interactions play a critical role in resonant charge transfer in molecular tunnel junctions (MTJs). Only when such interactions are taken into account, does it become possible to obtain the correct values of the turn-on threshold voltage in the current-voltage characteristics observed in experiment. In addition, we predict the emission of photons from MTJs with a large quantum yield $\sim 10^{-2}$ as a result of the excitation of surface plasmons upon the application of a voltage across the junction. Finally, we discuss physical conditions, which are necessary for the experimental observation of this phenomenon.

DOI: 10.1103/PhysRevB.81.035404 PACS number(s): 73.63.−b, 71.45.Gm, 81.07.Nb

One of the fundamental concepts in surface science is an attractive interaction of an external charge with a metallic surface, which results from the polarization of the metallic electrons, or on the quantum mechanical level, is due to collective electronic excitations—surface plasmons.[1] In the long wavelength limit, and at a sufficiently large distance z from the metal surface, the quantum description of plasmon excitations reduces to the classical notion of the image potential, $-1/4z$. In a system of classical charges, the effect of the image potential can be taken into account by considering the electrostatic interactions of the point charges with their images, and then introducing the corresponding term into the Hamiltonian of the quantum system. In the case of neutral atoms and molecules, changes in the energy levels are quite small.[2] It is expected that in charged molecules this effect will be more pronounced. In particular, in recent works by Kubatkin *et al.*[3] and Hedegård and Bjørnholm,[4] electron localization near the metal-molecule interface in MTJs was considered and attributed to the effect of the classical image potential.

In the second half of the last century, image-potential effects, including the dynamical corrections due to surface plasmons, were the focus of intensive experimental and theoretical investigations.[5–8] The renewed interest in electron-plasmon interactions at surfaces comes from recent advances in experimental investigations of surface nanostructures, including single molecules using surface plasmon resonance,[9] surface enhanced Raman spectroscopy,[10] scanning tunneling microscopy,[11] and molecular electronics.[12] It was the realization of the critical importance of surface plasmon effects in charge transport through molecular adsorbates that motivated the current work.

The dynamical image potential effects due to the interaction of an electron with surface plasmons have been considered by several researchers in the context of vacuum tunneling. In particular, Persson and Baratoff showed that electron-plasmon interactions substantially modify the shape of the tunneling barrier in vacuum, which is dependent upon the energy of the tunneling electron.[13] However, in the case of charge transport through a molecule, the situation is complicated by the fact that the charge carrier interacts with both surface plasmons and molecule in the course of the quantum transition. Such phenomena have not been considered before and, as it is shown in this article, have important implications for understanding the fundamental mechanisms of charge transport in molecular tunnel junctions (MTJs).

The purpose of this work is to show that electron-plasmon interactions play a crucial role in resonant charge transfer in MTJs. The challenge for the theory is to take into account the interactions between the two quantum systems—electron (hole) plus the molecule and the surface plasmons on the metallic electrodes. By developing a quantum mechanical approach to solve for the eigenvalues and wave functions of the combined system, we find that although the interaction of an electron (hole) with each of the N_{sp} surface plasmons is weak ($N_{sp}\sim$ number of surface atoms, $N_{sp}\to\infty$), the net effect of interaction with all surface plasmons is finite, which results in a substantial modification of the energy levels, and appreciable mixing of electron-plasmon excitations.

The mechanism of resonant tunneling in MTJs involves the electron ε^- or hole ε^+ molecular charged states defined as $\varepsilon_n^-=E_n^--E^0$ or $\varepsilon_n^+=E^0-E_n^+$, where E_n^- and E_n^+ are the total energies of negative and positive molecular ions in an electronic state n, and E^0 is the total energy of the neutral molecule M^0 in its ground electronic state.[14–16] A large increase in current takes place at V_{th} when either the ε^- or ε^+ enter the "current energy window" $[E_F-eV,E_F]$, see Fig. 1. Molecular resonant conduction is based on independent transitions of charge carriers (electrons, holes) via charged states of the molecule (M^-,M^+).[16] If the molecule is attached to metallic electrodes, it is expected that the effect of polarization interaction of the charged states (M^-,M^+) with the metallic electrodes will be much stronger than that for the states of the neutral molecule M^0.

We start with Hamiltonian of the system defined in Ref. 13,

$$H=H_e+H_{sp}(\{X_{\mathbf{q}}\})+H_{int}(\mathbf{r},\{X_{\mathbf{q}}\}), \tag{1}$$

where $H_e=\mathbf{p}^2/2m_e+U(\mathbf{r})$ is the Hamiltonian of the electron (hole) on the molecule with one-electron eigenstates (ε_n,ϕ_n): $H\phi_n=\varepsilon\phi_n$, and $U(\mathbf{r})$ is the electron (hole) potential, which also includes the external electric field. H_{sp} is the surface plasmon Hamiltonian, $H_{sp}(X_{\mathbf{q}})=\Sigma_{\mathbf{q}}\hbar\omega_{\mathbf{q}}(b_{\mathbf{q}}^{\dagger}b_{\mathbf{q}}+1/2)$, where $X_{\mathbf{q}}$ is the coordinate of the plasmon mode with momentum $\mathbf{q}$, and the total number of plasmon modes is N_{sp}. The interac-

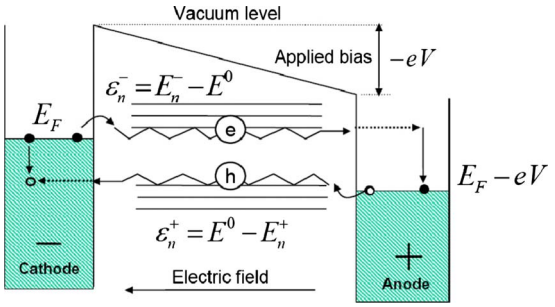

FIG. 1. (Color online) Schematic of energy diagram of the MTJ. The resonant electron ε_n^- and hole ε_n^+ energy levels are shown.

tion between an electron (hole) and the surface plasmons is described as $H_{int}=\Sigma_{\mathbf{q}}C_{\mathbf{q}}e^{-qz}(b_{\mathbf{q}}e^{i\mathbf{qr}_\parallel}+\text{H.c.})$, where the electron coordinate is $\mathbf{r}=(\mathbf{r}_\parallel,z)$, and z is the distance from the metallic surface as defined in Ref. 5. To extract the explicit expression for the classical image potential $U_{im}=-e^2/4z$ from H_{int}, and to include it into H_e, the plasmon coordinates $X_{\mathbf{q}}$ are transformed as

$$X_{\mathbf{q}}^* = X_{\mathbf{q}} + \delta X_{\mathbf{q}}, \quad \delta X_{\mathbf{q}} = C_{\mathbf{q}}e^{-qz}\sqrt{\frac{2}{\hbar m\omega_{\mathbf{q}}^3}}\begin{bmatrix}\cos(\mathbf{qr}_\parallel)\\ \sin(\mathbf{qr}_\parallel)\end{bmatrix}, \quad (2)$$

where $\cos(\mathbf{qr}_\parallel)$ and $\sin(\mathbf{qr}_\parallel)$ correspond to even and odd plasmon modes. The coefficient $C_{\mathbf{q}}$ is defined in Ref. 13, $C_{\mathbf{q}}\sim 1/\sqrt{N_{sp}}$.

The transformed total Hamiltonian is

$$H = \tilde{H}_e + H_{sp}(\{X_{\mathbf{q}}^*(\mathbf{r})\}), \quad \tilde{H}_e = H_e + U_{im}(z),$$

$$U_{im}(z) = -\sum_{\mathbf{q}}\frac{C_{\mathbf{q}}^2}{\hbar\omega_{\mathbf{q}}}e^{-2qz} = -\frac{e^2}{4z}. \quad (3)$$

Once transformed, the Hamiltonian becomes a sum of electronic and plasmon parts only, $H=\tilde{H}_e+H_{sp}$, with corresponding eigenfunctions $\phi(\mathbf{r})$ and $\chi(\{X_{\mathbf{q}}^*\})=\Pi_{\mathbf{q}}(X_{\mathbf{q}}^*)$.

By solving the Schrodinger equation with the electronic Hamiltonian $\tilde{H}_e$, which is the first step in our scheme, we immediately find the important physical consequence of the polarization interaction. The energy of the molecular resonant charged states are shifted with respect to the Fermi levels of the electrodes such that the predicted threshold voltage in the *I-V* characteristics becomes close to the experimental value. In particular, recent experiments on molecular rectification[17] measured a threshold voltage of ~1 eV, but the value predicted by using density functional theory alone is $V_{th}\approx 2(E_F-\varepsilon_1^+)=2.6$ eV, where ε_1^+ is the lowest-hole energy level. An additional shift of the energy levels due to the polarization interaction with the electrodes was calculated to be −0.75 eV, thus bringing the value of $V_{th}\approx 2(E_F-\varepsilon_1^+ + E_{im})=1.1$ eV close to that observed in experiment.[17]

However, the major effect of the electron-plasmon interactions is in the dependence of the transformed plasmon coordinates $X_{\mathbf{q}}^*$ on the electron coordinate $\mathbf{r}$. If the total wave function is written as $\Psi(\mathbf{r},\{X_{\mathbf{q}}^*\})=\phi(\mathbf{r})\chi(\{X_{\mathbf{q}}^*(\mathbf{r})\})$, then the Schrodinger equation is

$$(\tilde{H}_e\phi)\chi + \phi(H_{sp}\chi) - \phi\frac{\hbar^2}{2m}\boldsymbol{\nabla}\cdot\boldsymbol{\nabla}\chi - \frac{\hbar^2}{2m}\boldsymbol{\nabla}\phi\cdot\boldsymbol{\nabla}\chi = E\phi\chi, \quad (4)$$

where E is the eigenvalue of the electron-plasmon system. In the following, we drop the asterisk and use $X_{\mathbf{q}}$ for the shifted plasmon coordinate $X_{\mathbf{q}}^*$. The eigenvalues and eigenfunctions of Eq. (4) are sought by the variational method where the eigenfunctions Ψ are represented as linear combination of the products of electron and plasmon wave functions which include interactions with the left and right electrodes separated by distance L. The variational problem can in principle be solved within any molecular electronic structure method. However, in order to clarify the fundamental physics of electron-plasmon interactions in MTJs during resonant tunneling, we consider a very simple tight-binding model of MTJ—a molecular chain, placed along the z axis between two parallel gold electrodes biased by the voltage applied across the junction.

The tight-binding Hamiltonian is

$$H_{TB} = \sum_{i=1}^{N}\varepsilon_i a_i^\dagger a_i + h_0(a_i^\dagger a_{i+1} + \text{H.c.}), \quad (5)$$

where h_0 is the hopping integral and ε_i are the renormalized on-site energies, which include both the image potential and the external electric field $\mathcal{E}_z$ such that

$$\varepsilon_i = U_{im}(z_i) + U_{im}(L-z_i) - q\mathcal{E}_z z_i, \quad (6)$$

where $q=\{-e,+e\}$ is the electron or hole charge. Within the tight-binding model, the variational wave function is

$$\Psi = \sum_{i=1}^{N}B_i^0\Psi_i^0 + \sum_{i=1}^{N}\sum_{\mathbf{q}_L}B_i^{\mathbf{q}_L}\Psi_i^{\mathbf{q}_L} + \sum_{i=1}^{N}\sum_{\mathbf{q}_R}B_i^{\mathbf{q}_R}\Psi_i^{\mathbf{q}_R}, \quad (7)$$

where the basis functions on site i are

$$\Psi_i^0 = \varphi_i\prod_{\mathbf{q}_L}\chi_0(X_{\mathbf{q}_L}(z_i))\prod_{\mathbf{q}_R}\chi_0(X_{\mathbf{q}_R}(L-z_i)), \quad (8)$$

$$\Psi_i^{\mathbf{q}_L} = \varphi_i\chi_1(X_{\mathbf{q}_L}(z_i))\prod_{\mathbf{q}_L'\neq\mathbf{q}_L}\chi_0(X_{\mathbf{q}_L'}(z_i))\prod_{\mathbf{q}_R}\chi_0(X_{\mathbf{q}_R}(L-z_i)). \quad (9)$$

The expression for $\Psi_i^{\mathbf{q}_R}$ is similar to Eq. (9). Here, φ_i is the original electron (hole) orbital on site i, where $i=1,\ldots N$, and Ψ_i^0 is the electron-plasmon wave function on site i without plasmon excitation, $\Psi_i^{\mathbf{q}_L}$—with the excitation of the plasmon $\mathbf{q}_L$ in the left electrode.

The dimension of the combined electron-plasmon basis [Eqs. (8) and (9)] is $N(2N_{sp}+1)$, and the tight-binding Hamiltonian matrix in this basis is sparse. The matrix elements $\langle\Psi_i^{\mathbf{q}_L}|H|\Psi\rangle\sim\delta_{\mathbf{q}_L,\mathbf{q}_L'}$, because for $\mathbf{q}_L\neq\mathbf{q}_L'$ they are proportional to $1/N_{sp}\to 0$ (the number of surface plasmons N_{sp} is equal to the number of elemental surface unit cells in the entire crystal).

The diagonal matrix elements are $\langle\Psi_i^0|H|\Psi_i^0\rangle=\varepsilon_i$ and $\langle\Psi_i^{\mathbf{q}_L}|H|\Psi_i^{\mathbf{q}_L}\rangle=\varepsilon_i+\hbar\omega_{\mathbf{q}_L}$. The nondiagonal matrix element $\langle\Psi_i^0|H|\Psi_{i+1}^0\rangle$ is calculated by using expression (8) for Ψ_i^0,

and expanding the plasmon wave function $\chi_0(X_{\mathbf{q}_{L,R}}(z_{i+1}))$ in a Taylor series in the vicinity of $X_{\mathbf{q}_{L,R}}(z_i)$. Keeping only terms $\sim 1/N_{sp}$, we obtain

$$\langle \Psi_i^0 | H | \Psi_{i+1}^0 \rangle = \tilde{h}_{i,i+1}, \tag{10}$$

$$\tilde{h}_{i,i+1} = h_0[1 - \Theta(z_i, z_{i+1})/2][1 - \Theta(L - z_i, L - z_{i+1})/2], \tag{11}$$

$$\Theta(z_i, z_{i+1}) = \frac{1}{\hbar \bar{\omega}_{sp}} \left(\frac{e^2}{4z_i} + \frac{e^2}{4z_{i+1}} - \frac{e^2}{z_i + z_{i+1}} \right). \tag{12}$$

Here, $\bar{\omega}_{sp}$ is the surface plasmon frequency averaged over the plasmon spectrum, and $\tilde{h}_{i,i+1}$ are the renormalized hopping integrals. Another nondiagonal matrix element $\langle \Psi_i^{\mathbf{q}_L} | H | \Psi_{i+1}^{\mathbf{q}_L} \rangle$ is different from $\langle \Psi_i^0 | H | \Psi_{i+1}^0 \rangle$ by additional terms $\sim 1/N_{sp}$, which can be neglected. Therefore, we obtain

$$\langle \Psi_i^{\mathbf{q}_L} | H | \Psi_{i+1}^{\mathbf{q}_L} \rangle \simeq \tilde{h}_{i,i+1}. \tag{13}$$

The nondiagonal matrix elements $\langle \Psi_i^0 | H | \Psi_{i+1}^0 \rangle$ and $\langle \Psi_i^{\mathbf{q}_L} | H | \Psi_{i+1}^{\mathbf{q}_L} \rangle$ conserve the number of plasmons in the system. The matrix elements that change the number of plasmons by one are $\langle \Psi_i^0 | H | \Psi_{i+1}^{\mathbf{q}_{L,R}} \rangle = t_{i,i+1}(\mathbf{q}_{L,R})$, where

$$t_{i,i+1}(\mathbf{q}_L) = \tilde{h}_{i,i+1}(e^{-q_L z_{i+1}} - e^{-q_L z_i}) \frac{C_{\mathbf{q}_L}}{\hbar \omega_{\mathbf{q}_L}},$$

$$t_{i,i+1}(\mathbf{q}_R) = \tilde{h}_{i,i+1}(e^{-q_R(L - z_{i+1})} - e^{-q_R(L - z_i)}) \frac{C_{\mathbf{q}_R}}{\hbar \omega_{\mathbf{q}_R}}. \tag{14}$$

In order to find the eigenvalues of the tight-binding electron-plasmon matrix, the system of N equations $\langle \Psi_i^{\mathbf{q}_{L,R}} | H - EI | \Psi \rangle = 0$ for N coefficients $B_i^{\mathbf{q}_{L,R}}$ is solved. The coefficients $B_i^{\mathbf{q}_{L,R}}$ are then expressed as a linear combination of $\{B_i^0\}$, $i = 1, \ldots N$. As a consequence, $B_i^{\mathbf{q}_{L,R}}$ depend on energy E. To obtain the system for coefficients B_i^0, the coefficients $B_i^{\mathbf{q}_{L,R}}$ are substituted into the system of equations $\langle \Psi_i^0 | H - EI | \Psi \rangle = 0$, where each equation contains the sum $\Sigma_{j=1}^N \Sigma_{\mathbf{q}_{L,R}} B_j^{\mathbf{q}_{L,R}} t_{j,j+1}(\mathbf{q}_{L,R})$. Because both $t_{j,j+1}$ and $B_j^{\mathbf{q}_{L,R}}$ are proportional to $1/\sqrt{N_{sp}}$, and since the summation over $\mathbf{q}_{L,R}$ involves N_{sp} terms, the sum is the finite linear combination of B_j^0. The coefficient matrix of the system is energy dependent; therefore, the solution of the secular equation results in $2N$ eigenvalues of E.

The physical meaning of the appearance of the extra N eigenvalues is that they describe the one-plasmon excitations due to the electron-plasmon interactions in the course of electron hopping between neighboring centers i and $i+1$, i.e., during the motion of the electron along the molecule. When such excitations are switched off by setting $t_{i,i+1} = 0$, the eigenvalues of the electron-plasmon system become $\{E_\nu(\tilde{h}), E_\nu(\tilde{h}) + \hbar \bar{\omega}_{sp}\}$, $\nu = 1, \ldots N$.

In order to estimate the magnitude of the electron-plasmon effects in MTJs, we consider an analytically solvable tight-binding model consisting of two centers that are placed between the gold electrodes. Then, the tight-binding electron-plasmon eigenvalues are

$$E_{1,2,3,4} = \frac{\varepsilon_1 + \varepsilon_2 + \hbar \bar{\omega}_{sp}}{2} \pm \sqrt{\left(\frac{\varepsilon_1 - \varepsilon_2}{2} \right)^2 + \left(\frac{\hbar \bar{\omega}_{sp}}{2} \right)^2 + \tilde{h}_{12}^2 (1 + \Theta_{12}) \pm \hbar \bar{\omega}_{sp} \sqrt{\left(\frac{\varepsilon_1 - \varepsilon_2}{2} \right)^2 + \tilde{h}_{12}^2}}, \tag{15}$$

where $\Theta_{12} = \Theta(z_1, z_2) + \Theta(L - z_1, L - z_2)$. The eigenvalues without electron-plasmon excitations, $t_{i,i+1} = 0$, are

$$E_{1,2}^{(0)} = \frac{\varepsilon_1 + \varepsilon_2}{2} \pm \sqrt{\left(\frac{\varepsilon_1 - \varepsilon_2}{2} \right)^2 + \tilde{h}_{12}^2},$$

$$E_{3,4}^{(0)} = E_{1,2}^{(0)} + \hbar \omega_s, \tag{16}$$

where the renormalized hopping integral $\tilde{h}_{12}$ and on-site energies $\varepsilon_1, \varepsilon_2$ are defined by expressions (11) and (6), respectively. The four eigenvalues E_{1-4} are shown in Fig. 2 as a function of the hopping integral h_0 for the case of gold electrodes, $\hbar \bar{\omega}_{sp} \approx 2.5$ eV.[18] $E_{1-4}^{(0)}$ are also shown for comparison as dashed lines. The geometry of the junction is the following: lattice sites are situated symmetrically with respect to two surfaces; the intersite distance is $z_2 - z_1 = 2$ Å and the distance between the metallic surface and the nearest lattice site is $z_1 = L - z_2 = 1.1$ Å.

Due to nonzero matrix elements $t_{i,i+1}(\mathbf{q}_{L,R})$ the plasmonless states $E_{1,2}^{(0)}$ are mixed with the states $E_{3,4}^{(0)}$ containing plasmon excitations. This is most clearly seen from Fig. 2 where the states $E_2^{(0)}$ and $E_3^{(0)}$ intersect at $h_0 \sim 1.5$ eV, and where, due to $t_{i,i+1}(\mathbf{q}_{L,R})$, they split. The wave functions of the new states corresponding to E_i contain plasmonless and single plasmon components. Therefore, there is a nonzero probability of a surface plasmon excitation in the metallic electrodes during an electron (hole) resonant tunneling transition via this level.

Let us then consider the process of plasmon excitation in either anode or cathode during resonant electron transfer via the resonant level E_1, which is in the current energy window $[E_F, E_F - eV]$ at the applied voltage V, see Fig. 1. Due to the conservation of energy, a plasmon can only be emitted if $eV \geq E_F - E_1 + \hbar \bar{\omega}_{sp}$. The probability amplitude of an electron transition from the cathode (state i, left electrode) to the anode (state f, right electrode) with the excitation of a surface plasmon $\mathbf{q}_a$ at the anode is

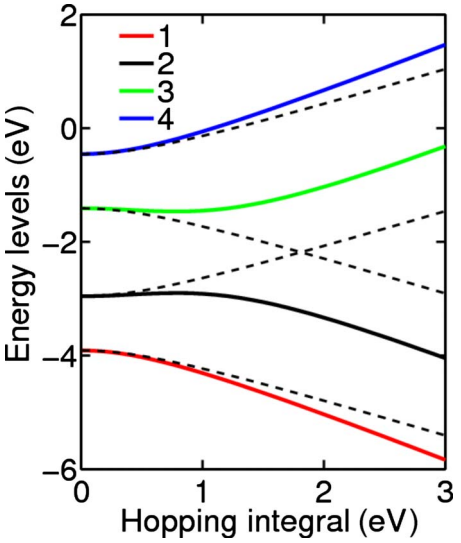

FIG. 2. (Color online) Electron-plasmon energy levels versus hopping integral h_0 for the two-site, tight-binding model (the bias voltage is 2 V). Solid lines are the levels E_{1-4} Eq. (15), dashed lines are the levels $E^{(0)}_{1-4}$ Eq. (16) with electron-plasmon excitations turned off. At $h_0 \sim 1$ eV, energy levels E_2 and E_3 consist of a mixture of states $E^{(0)}_2$ and $E^{(0)}_3$ (with and without plasmons).

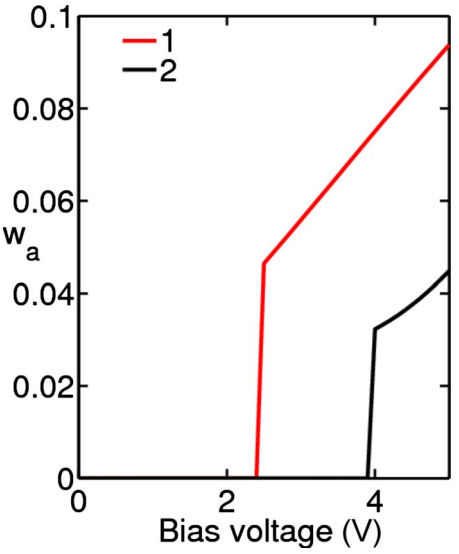

FIG. 3. (Color online) Probability ratio of the resonant transitions with and without plasmon excitation on the anode for the two lowest energy levels E_1 and E_2 as a function of bias voltage at $h_0 = 1$ eV.

$$A^{\mathbf{q}_a}_{if} = \frac{\langle \Phi^{\mathbf{q}_a}_f | U_a | \Psi_1 \rangle \langle \Psi_1 | U_c | \Phi^c_i \rangle}{\varepsilon_i - E_1 + i\Gamma}, \tag{17}$$

where the wave functions of the final and initial states are

$$\Phi^{\mathbf{q}_a}_f = \phi^a_e(\mathbf{r}, \varepsilon_f) \chi^{\mathbf{q}_a}_1 \Pi_{\mathbf{q}'_a \neq \mathbf{q}_a} \chi^{\mathbf{q}'_a}_0 \Pi_{\mathbf{q}_c} \chi^{\mathbf{q}_c}_0,$$

$$\Phi^c_i = \phi^c_e(\mathbf{r}, \varepsilon_i) \Pi_{\mathbf{q}_a} \chi^{\mathbf{q}_a}_0 \Pi_{\mathbf{q}_c} \chi^{\mathbf{q}_c}_0,$$

$U_{c,a}$, and $\phi^{c,a}_e$ are the one-particle potentials and wave functions respectively of electrons inside the cathode and anode, and Ψ_1 is the total wave function of the electron resonant state with energy E_1, including both electron and plasmon coordinates as defined by Eqs. (8) and (9). The greatest contribution to the matrix element $\langle \Phi^{\mathbf{q}_a}_f | U_a | \Psi_1 \rangle$ is due to the center N closest to the anode, $\phi(z - z_N)$, and in the cathode matrix element $\langle \Psi_1 | U_c | \Phi^c_i \rangle$—from the center 1, $\phi(z - z_1)$. Then, using Eqs. (8), (9), and (17), the transition amplitude becomes $A^{\mathbf{q}_a}_{if} = D B^{\mathbf{q}_a}_N B^0_1$, where D is a constant. The probability amplitude for the transition without plasmon excitation is $A^0_{if} = D B^0_N B^0_1$. Then, the probability ratio for the transition with and without excitation of a surface plasmon mode $\mathbf{q}_a$ on the anode $w^{\mathbf{q}_a} = |B^{\mathbf{q}_a}_N|^2 / |B^0_N|^2 \sim 1/N_{sp}$ is very small. However, the probability ratio for excitation of *any* plasmon mode on the anode, $w_a = \Sigma_{\mathbf{q}_a} w^{\mathbf{q}_a}$, is a finite quantity $w_a \propto \Theta(z_{N-1}, z_N)$.

The probability ratio w_a as a function of the applied bias is shown in Fig. 3. The first plasmon excitation occurs at 2.5 V, the voltage corresponding to the surface plasmon frequency of gold,[18] during resonant tunneling via the first energy level E_1. The second excitation occurs at 4 V via the second energy level E_2. As is seen from Fig. 3, several percent of tunneling events occur with excitation of surface plasmons.

In this work we predict the excitation of surface plasmons in the course of resonant tunneling current through the MTJ. The experimental confirmation can be an observation of photons emitted with frequency ω_{sp} at the molecule/electrode interface when the surface plasmons are transformed into photons at surface defects.[19] In principle, the excitation of surface plasmons by energetic electrons impinging the metallic surface, followed by photon emission, is possible without the presence of the molecule.[20–22] However, energy relaxation of an electron arriving with an energy above the Fermi energy of the metallic electrodes occurs via two competing processes: emission of plasmons or energy transfer to other metallic electrons in electron-electron collisions. Because the latter process is much more efficient than a direct emission of plasmons, the quantum yield of such a process in bare metals is very small ($\sim 10^{-6}$).[20–22] In contrast, the probability of plasmon emission during resonant transition of an electron and/or hole through the molecule is determined entirely by the magnitude of the electron-plasmon interaction; therefore, the quantum yield is several orders of magnitude higher. Another mechanism of photon emission in MTJs is due to direct electron excitation of the molecule by a tunneling electron. However, both theory[23] and experiment[24] show that the quantum yield of such a process is also very small, 10^{-7}–10^{-6}.

Resonant electron-plasmon interactions provide a plausible mechanism of photon emission in MTJs with a large quantum yield ($\sim 10^{-2}$). However, the experimental observation of such an effect requires the application of a large bias ($V \gtrsim \hbar\omega_{sp}/e \sim 2$–$3$ V), which is difficult to accomplish in standard experiments with MTJs due to the likelihood of damage to the molecule.[17] Two possibilities exist to circumvent this difficulty. It is known that the plasmon frequency is reduced in metal nanostructures, which may allow the observation of electron-plasmon photon emission at smaller

bias using an scanning tunneling microscope (STM) tip as one of the electrodes. The second possibility is to reduce the current through the molecule by introducing a vacuum gap between the molecule and one of the electrodes, which can also be realized using an STM.[25,26]

The authors thank NSF for financial support (Grants No. 0650028 and No. 0726842). L.A. is supported by the USF Presidential Graduate Fund. M.A.K. thanks RFFI for the financial support under the Grant No. 09-03-92474-MHKC.

[1] A. Zangwill, *Physics at Surfaces* (Cambridge University Press, Cambridge, England, 1988).
[2] K. Ganesan and K. T. Taylor, J. Phys. B **29**, 1293 (1996).
[3] S. Kubatkin, A. Danilov, M. Hjort, Jérôme Cornil, Jean-Luc Brédas, Nicolai Stuhr-Hansen, Per Hedegård, and Thomas Bjørnholm, Nature (London) **425**, 698 (2003).
[4] P. Hedegård and T. Bjørnholm, Chem. Phys. **319**, 350 (2005).
[5] N. D. Lang and W. Kohn, Phys. Rev. B **7**, 3541 (1973).
[6] G. Binnig, K. H. Frank, H. Fuchs, N. Garcia, B. Reihl, H. Rohrer, F. Salvan, and A. R. Williams, Phys. Rev. Lett. **55**, 991 (1985).
[7] K. Giesen, F. Hage, F. J. Himpsel, H. J. Riess, and W. Steinmann, Phys. Rev. Lett. **55**, 300 (1985).
[8] P. M. Echenique and J. B. Pendry, Prog. Surf. Sci. **32**, 111 (1989).
[9] J. C. Love, L. A. Estroff, J. K. Kriebel, R. G. Nuzzo, and G. M. Whitesides, Chem. Rev. **105**, 1103 (2005).
[10] S. M. Nie and S. R. Emery, Science **275**, 1102 (1997).
[11] G. Binnig, H. Rohrer, C. Gerber, and E. Weibel, Phys. Rev. Lett. **49**, 57 (1982).
[12] J. R. Heath and M. A. Ratner, Phys. Today **56**, 43 (2003).
[13] B. N. J. Persson and A. Baratoff, Phys. Rev. B **38**, 9616 (1988).
[14] S. Datta, *Quantum Transport: From Atom to Transistor* (Cambridge University Press, Cambridge, England, 2005).
[15] M. A. Kozhushner, V. S. Posvyanskii, and I. I. Oleynik, Chem. Phys. **319**, 368 (2005).
[16] I. I. Oleynik, M. A. Kozhushner, V. S. Posvyanskii, and L. Yu, Phys. Rev. Lett. **96**, 096803 (2006).
[17] I. Díez-Pérez, J. Hihath, Y. Lee, L. Yu, L. Adamska, M. A. Kozhushner, I. I. Oleynik, and N. J. Tao, Nat. Chem. **1**, 635 (2009).
[18] A. S. Barker, Jr., Phys. Rev. B **8**, 5418 (1973).
[19] R. A. Ferrell, Phys. Rev. **111**, 1214 (1958).
[20] J. K. Gimzewski, B. Reihl, J. H. Coombs, and R. R. Schlittler, Z. Phys. B **72**, 497 (1988).
[21] B. N. J. Persson and A. Baratoff, Phys. Rev. Lett. **68**, 3224 (1992).
[22] J. Lambe and S. L. McCarthy, Phys. Rev. Lett. **37**, 923 (1976).
[23] M. Galperin and A. Nitzan, Phys. Rev. Lett. **95**, 206802 (2005).
[24] S. W. Wu, G. V. Nazin, and W. Ho, Phys. Rev. B **77**, 205430 (2008).
[25] B. Xu and N. J. Tao, Science **301**, 1221 (2003).
[26] M. K. Ng, D. C. Lee, and L. P. Yu, J. Am. Chem. Soc. **124**, 11862 (2002).